Aerodynamics of cars
Drag reduction

Alessandro Talamelli

Johan Westin

Mekanik/KTH

1

Outline

☐ General remarks on drag of cars
- How to analyse drag

☐ Local origins of drag
- Individual details and their contribution to drag

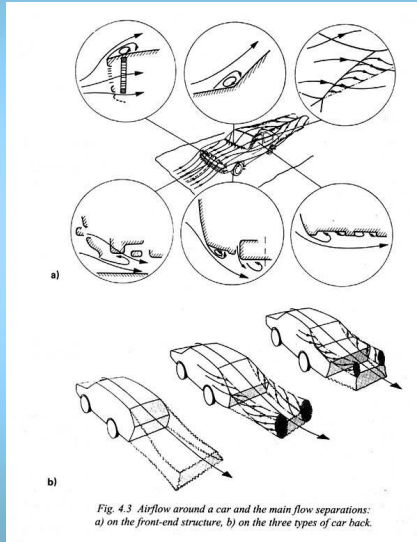☐ Ex. Optimisation of Opel Calibra

2

Flow around a car

Fig. 4.3 Airflow around a car and the main flow separations:
a) on the front-end structure, b) on the three types of car back.

- Car=relatively bluff body (c_D=0.25-0.45)
- Two types of separation
  1) Quasi 2D wakes
  2) Longitudinal vortices
- Rear end determines the wake structure
  1) Square back
  2) Fast back
  3) Notch back
- Underbody flow and wheels
- Interactions – ground effect

3

Drag and Lift

- Drag and lift normally related (lift generates drag)
- Wing theory: Drag = profile drag (form drag + friction drag) + induced drag (induced drag from wingtip vortices)

$$c_{Di} = k\frac{c_L^2}{\Lambda} \qquad \Lambda = \frac{b^2}{A_{plan}}$$

- Cars: low aspect ratio ($\Lambda \approx 0.4$)
- Interaction between tip vortices and the central flow

4

2

Approaches to analyse drag I

☐ Examine the physical mechanisms
- Identify separation regions
- Measure pressure and wall-shear stress
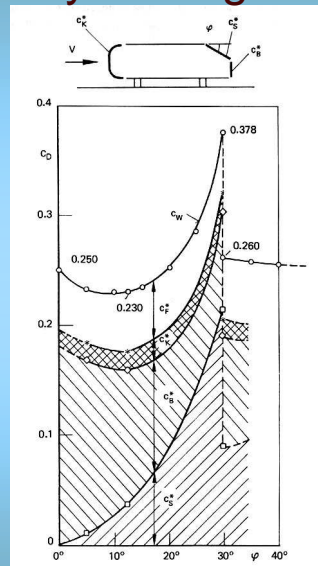- Drag obtained from surface integral
$$D = \oint p \sin \varphi \, dS + \oint \tau_w \cos \varphi \, dS$$
- Lot of experimental data needed (unrealistic)
- It is possible to find the local origins of drag

5

Approaches to analyse drag II

- Usually possible for simple bodies (see figure)
- Problem: in real cars different components interact!

6

Approaches to analyse drag III

□ Wake analysis

- Control volume approach + momentum theorem
- Energy assessment

!! Stationary wall: must subtract contribution from wall boundary layer

$$c_D A = \int_S (1 - c_{ptot})dS - \int_S \left(1 - \frac{u}{V}\right)^2 dS + \int_S \left[\left(\frac{v}{V}\right)^2 + \left(\frac{w}{V}\right)^2\right] dS$$

- Extensive measurements needed (costly)
- Need of traversing mechanism

Local origins of drag - Front end I

- Local separation less pronounced suction peak - increased drag
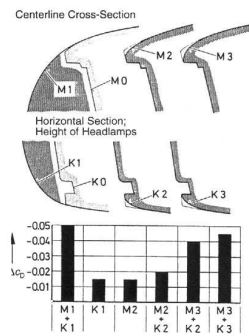
- Small edge radius enough to reduce local drag
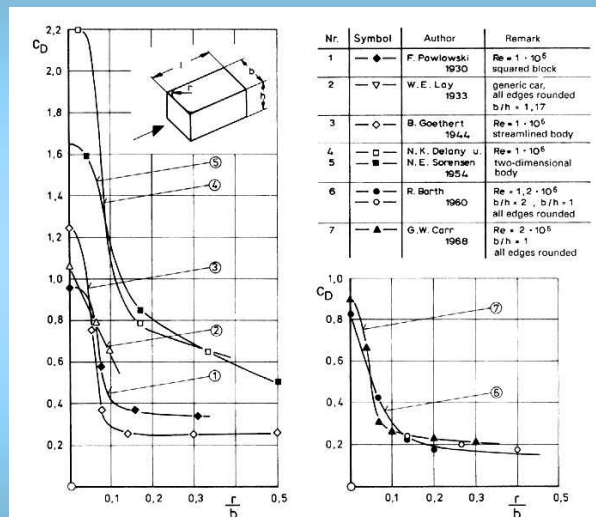
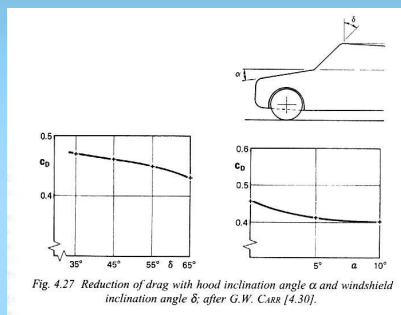Fig. 4.26 Influence of edge radius on the drag of squared blocks, compiled from [4.29].

Local origins of drag - Front end II

- Optimization of the front of Golf I
- Small radii can give significant drag reduction

Local origins of drag - Angle of hood and wind shield I

Fig. 4.27 Reduction of drag with hood inclination angle α and windshield inclination angle δ; after G.W. CARR [4.30].

- Drag reduction due to hood angle (α)saturates
  BUT: Combination effect of hood angle & front radius!
- Increased angle of wind shield (δ) can reduce drag
- $\delta \geq 60°$ => visibility and temperature problems
- indirect influence on drag:
  – Influence flow around A-pillar
  – Smaller suction peak at the junction to the roof

Local origins of drag - A-pillar

Figure 4.34 Vortex formation on the A-pillar, after ref. 4.33
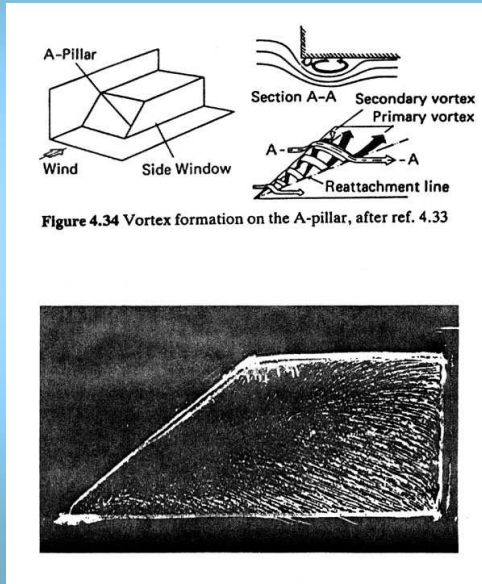
- 3D-separation (vortex)
- Wind noise
- Water and dirt deposition

Local origins of drag – Roof and Sides

- Mainly friction drag (flow is generally attached)
- Increased camber give larger radii =>reduced suction peaks
- Negative angle of roof => reduced wake
- Problems: large front area and/or smaller internal space

Local origins of drag Underbody flows

Fig. 4.12 Outward-spreading flow underneath a car.

- Complex flow
- Flow angles important
- Avoid obstacles (stagnation)
- Return of cooling air can influence

- Large improvement by rear panels
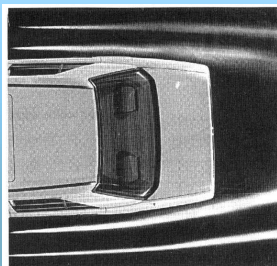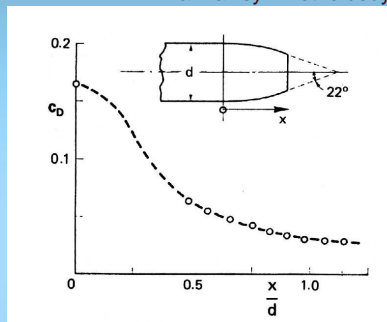- Also effect on lift
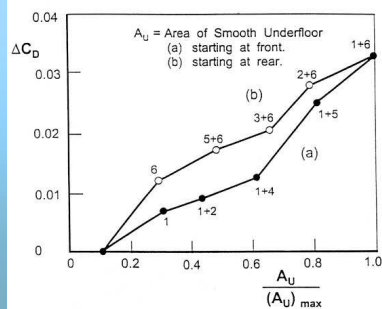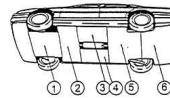
Ahmed (1999)

13

Local origins of drag - Rear End

Mair: axisymmetric body

☐Boat tailing

•Increase base pressure

•Reduce base area

•Minor improvements by further extension of the body (x/d > 5)

•Squareback vehicles: lower the roof
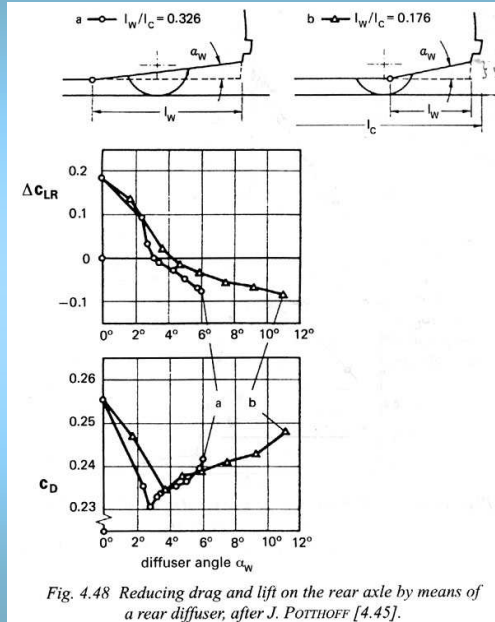
•Flow devices (Air intakes, wings)

Mercedes 190
Angle ca 10°

14

## Local origins of drag - Rear End II

☐ Boat-tailed underbody

- Requires smooth underbody
- Decreased drag for moderate diffuser angles
- Reduction in lift

Fig. 4.48 Reducing drag and lift on the rear axle by means of a rear diffuser, after J. POTTHOFF [4.45].
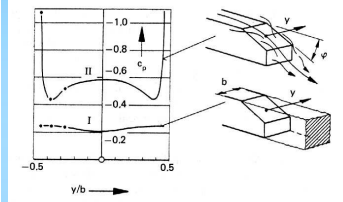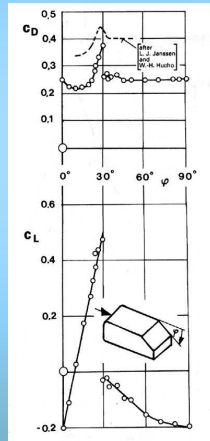
Local origins of drag - Rear End III

☐ Fastback/squareback

- Basic experiments =>understanding of rear end flow
- Drag due to strong side vortices
- Vortex break-up above critical slant angle
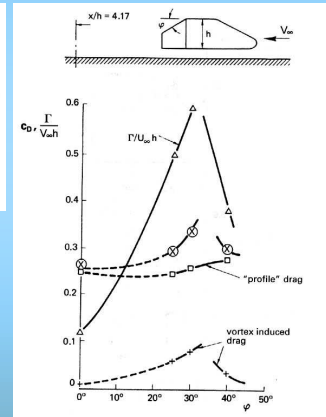
Morel (1976)   Bearman (1979)
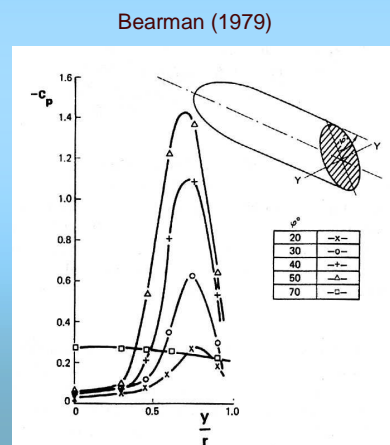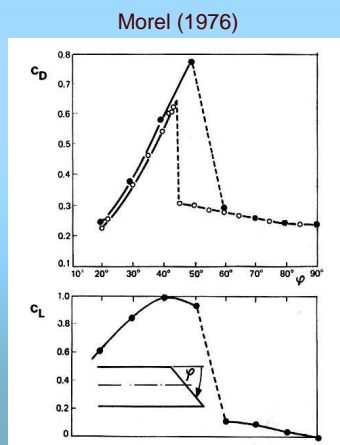
□Fastback/squareback

- Prismatic body near ground (qualitatively similar results)
- Critical slant angle ca 30°
- Drag minimum at $\varphi \approx 15°$ (coupé)

Morel (1976)

Bearman (1982)

17

□Fastback/squareback

Development of Golf I:
In-fluence of slant angle (φ)

- Bi-stable separation around critical angle ($\varphi \approx 30°$)
- $\varphi > 30°$: reduced drag and flow conditions similar to a square back
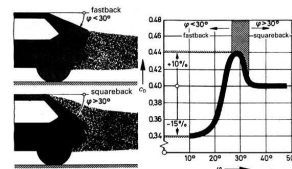- $\varphi > 30°$: Vortices are weaker and with opposite rotational direction than $\varphi < 30°$:

Fig. 4.55 Influence of slant angle φ on drag coefficient c_D and the flow regime in the rear of the car, measured during development of the Volkswagen Golf I (Rabbit), after L.J. JANSSEN and W.-H. HUCHO [4.33].
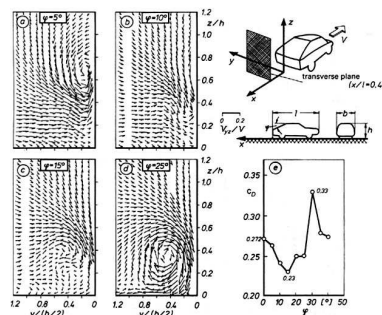
Fig. 4.8 Lateral-speed vectors and drag coefficient of a fastback, as a function of the slant angle φ, after S.R. AHMED [4.10].

18

9

Rounded rear edges

- Previous findings based on bodies with fairly sharp edges
- Rounded side edges => no fixed separation point
- Rounded rear => optimum base height more relevant than optimum slant angle
- Also: the base height influence by sloping side edges

19

□Notchback

- Interaction
  - quasi-2D separation
  - 3D vortices
- Several geometrical parameters
- Also influenced by
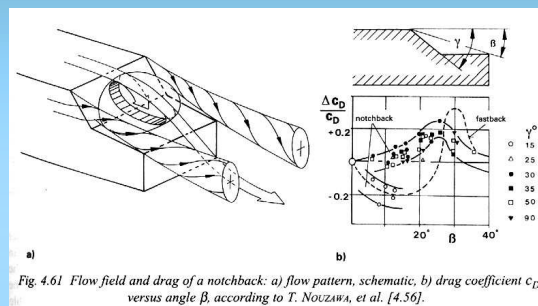 - Radius roof-window
  - Shape of C-pillar
  - Rear end of trunk

Fig. 4.61 Flow field and drag of a notchback: a) flow pattern, schematic, b) drag coefficient c_D versus angle β, according to T. NOUZAWA, et al. [4.56].

20

Flow in the "dead water region"

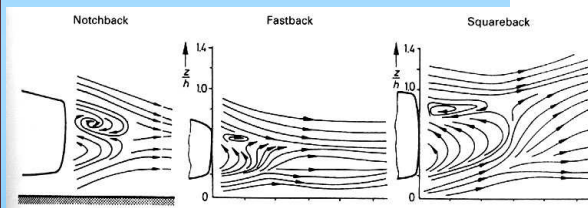- Counter rotating vortices (try to identify during PIV-lab)

Fig. 4.4 Contrarotating vortices in the dead water behind cars of different rear-end shape, after S.R. AHMED and W. BAUMERT [4.6].
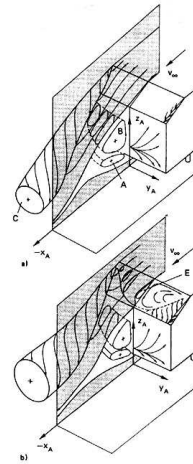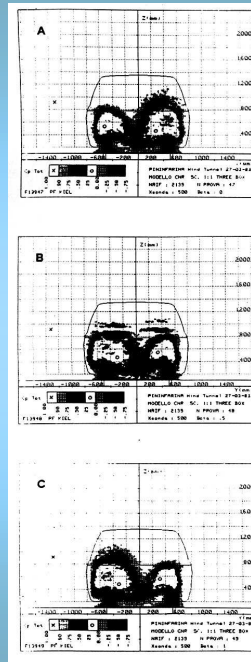
Fig. 4.10 Vortex system for a fastback with: a) low drag coefficient, b) high drag coefficient with φ = 30°, after S.R. AHMED, et al. [4.13].

21

Sensitivity to side wind

- Wake-analysis behind a notchback (Cogotti 1986)
- Total-pressure distribution show strong influence of small yaw angles (β=0, 0.5° & 1°)
- Bi-stable flow at β= 0.5°


22

Sensitivity to side wind II

- Attempt to explain asymmetric wake
  - A-pillar vortices interact with rear vortices
  - Very small yaw angles change the relative strength of A-pillar vortices

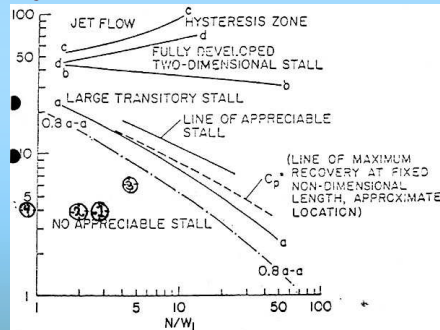- Symmetric flow pattern unlikely on three-box config.
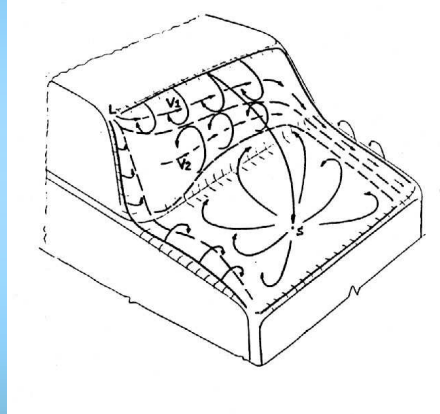
23

Mechanism of a 2D-diffuser

2-D Diffuser

- Pressure increases as long as flow not separated
- Max diffuser length longer for small diffuser angles

2θ

- Is the analogy with a 2D diffuser really correct?
- (Can explain reduced drag, but not reduced lift)
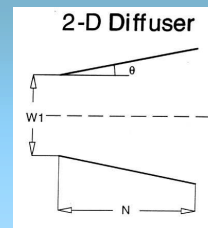
24

Aspects of underbody diffuser

☐ Rear end underbody diffuser brings up the velocity below the car (normally reduces lift)

☐ Higher velocity below the car changes flow angles around the wheels

- Reduced drag due to the wheels
- Requires a smooth underbody to avoid drag from obstacles

☐ Underbody diffuser reduces the base area of the vehicle (can reduce drag)

25

Underbody shaped for downforce I

☐ Ferrari 360 Modena

- "Venturi-tunnel" for max downforce
- Smooth underbody
- No spoilers
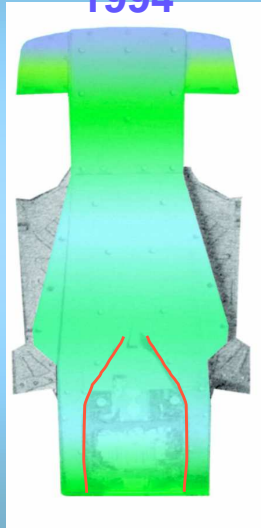- 5400 hours in wind-tunnel (source: Teknikens Värld 11/99)

Il fondo completamente carenato facilita e regolarizza il flusso di aria nella parte inferiore della vettura.
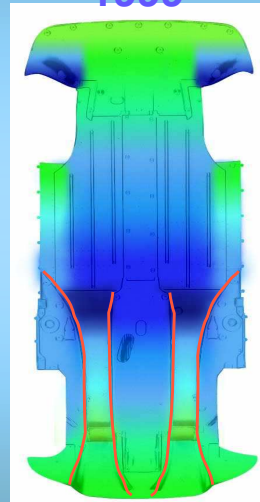
26

Underbody shaped for downforce I

1994

1999

F355

360 Modena

27

Wheels

- Up to 50% of the drag of a streamlined car
- Wheels are not streamlined
  - 3 vortex pairs
  - Influenced by ground and rotation
- Local flow is yawed (≈15°)
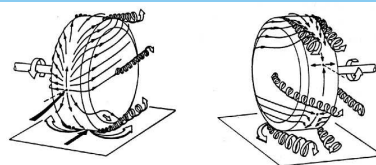 - Separation on the outer side
  - Water drops sucked out

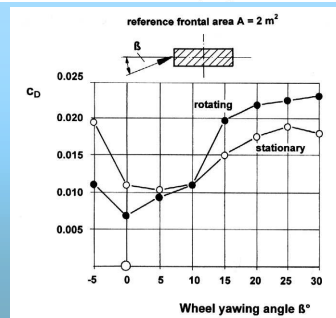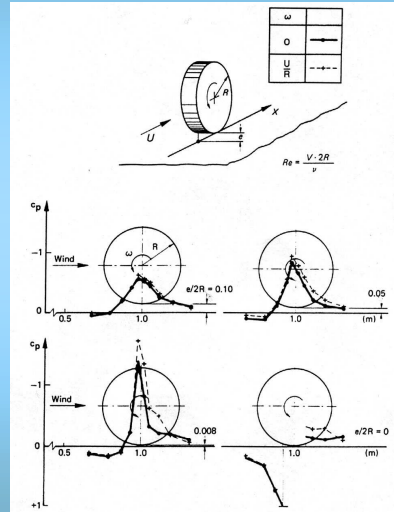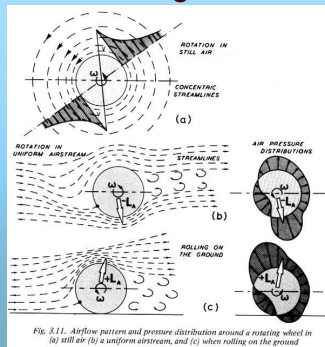*Fig. 4.72 Flow pattern of a wheel rolling on the ground, after E. MERCKER and H. BERNEBURG [4.61].*

reference frontal area A = 2 m²

c_D

0.025

0.020 — rotating

0.015 — stationary

0.010

0.005

-5   0   5   10   15   20   25   30

Wheel yawing angle ß°

28

Wheels (contd)

- Force on a rotating wheel changes sign when contact with ground
- Lift force due to wheel rotation for a free-standing wheel

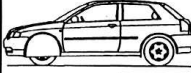Fig. 3.11. Airflow pattern and pressure distribution around a rotating wheel in (a) still air (b) a uniform airstream, and (c) when rolling on the ground
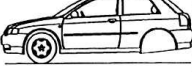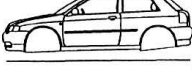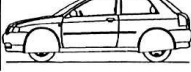
Wheels (contd)

- How does the flow in the wheel-housings look like?

- Wheel-housings
  - Smaller=better
  - Both lift and drag reduced
  - Largest effect on lift (see e.g. Cogotti 1983)
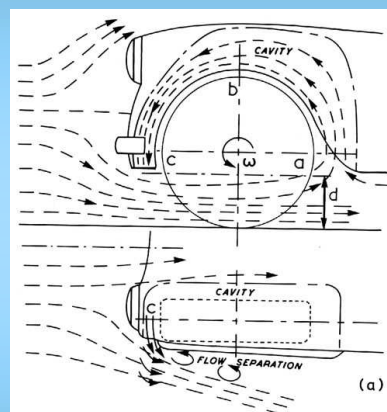
Influence of wheels on Audi A3

configurations without wheels (without wheels and wheel arches covered)		c_D	difference	c_D		conf. with wheel arches covered (only wheel arches covered)
	Δc_D		<- ->		Δc_D	
	Ref.	0.316	0.000	0.316	Ref.	
	0.042	0.274	0.029	0.303	0.013	
	0.057	0.259	0.051	0.310	0.006	
	0.102	0.214	0.080	0.294	0.022	

- 30-35% of drag due to wheels + wheel arches
- Ca 25% only due to wheels

From Pfadenhauer,
Wickern & Zwicker (1996)   31

Spoilers

☐ Front spoiler
  + Reduced drag
  + Reduced front axle lift
  + Improved cooling air flow
- Reduced flow rate under the car
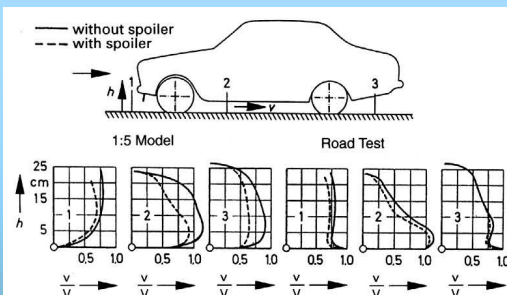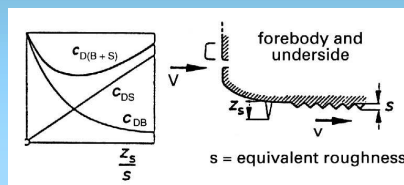- Low pressure region behind the spoiler
- Optimization needed

$c_{D(B+S)}$ c_{DS} c_{DB} $\dfrac{z_s}{s}$

forebody and underside z_s s v s = equivalent roughness

without spoiler
with spoiler

1:5 Model   Road Test

Fig. 4.78 Velocity distribution underneath a car with and without front spoiler, after C. KRAMER, et al. [4.65].

Hucho (1998)

16

☐ Rear spoiler

+ Reduced drag (sometimes)

+ Reduce rear axle lift

- Higher c_P in front of the spoiler

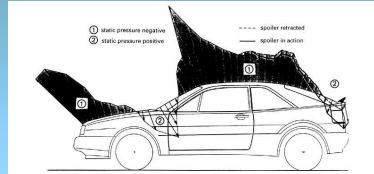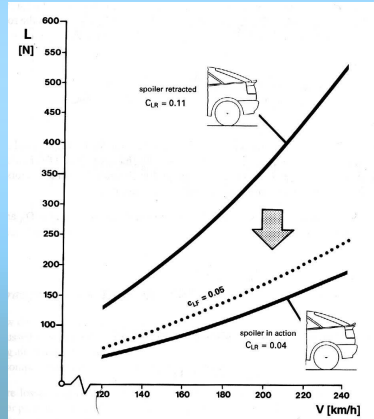- Increased spoiler height increases the lift, but also drag

Fig. 4.91 Change in pressure distribution around the Volkswagen Corrado with the addition of a retractable rear spoiler, after H. SCHUSTER and R. HORN [4.72].

33

Miscellaneous

- Cooling air flow: $\Delta c_D \approx 0.02\text{-}0.06$

- Side mirrors: $\Delta c_D \approx 0.01$

- Antenna: $\Delta c_D \approx 0.001$

- Roof racks: up to 30-40% increase in c_D
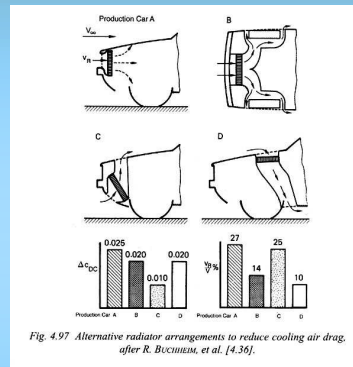
- Ski box: Why are they shaped in this way??

Fig. 4.97 Alternative radiator arrangements to reduce cooling air drag, after R. BUCHHEIM, et al. [4.36].

34

Potential fields for drag reduction

☐ More focus on underbody and wheels
☐ Active reduction of the dead-water region
  - Base bleed
☐ Separation control
  - Boundary layer suction?

35

Discrepancies in c_D

☐ Different c_D depending on equipment
  - Tire width
  - Engine type (cooling air flow)
  - Ground clearance (load dependent)
  - Angle of attack (load dependent)
  - Additional spoilers etc.

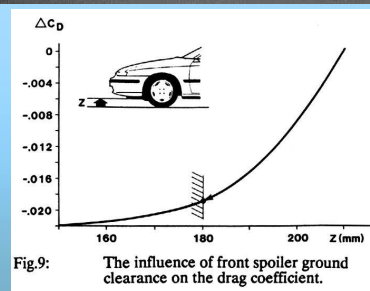☐ Official c_D values "corrected"

36

Aerodynamic optimization of Opel Calibra

- Front spoiler height optimization
  - Determined by minimum ground clearance

From Emmelmann et al (1990)

Fig.9: The influence of front spoiler ground clearance on the drag coefficient.

37

- Rear end optimization (1:5 scale model)

- Rear end tapering
- Decklid height optimization
  - Interdependent effect of decklif height and rear end tapering
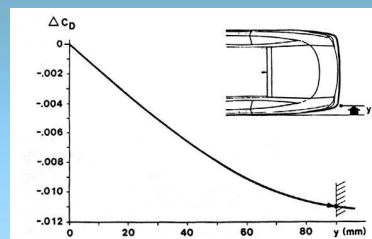 - Large number of parameter tests needed

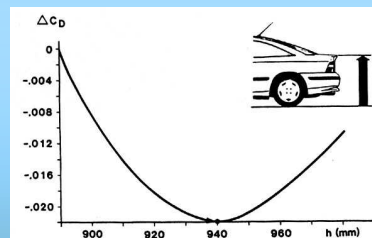Fig.10: The influence of rear end taper on the drag coefficient.

Fig.11: The influence of decklid height on the drag coefficient.

38

- $c_D \approx 0.28$ at this time
- Wake analysis (total pressure) and flow vis.
  - No noticeable tip vortices
  - "Ears" due to A-pillars
  - Wide wake close to ground
  - 30° flow angle at front wheels
- Drag reduction by
  - Reduced spoiler height in the centre
  - Increased spoiler height in front of wheels
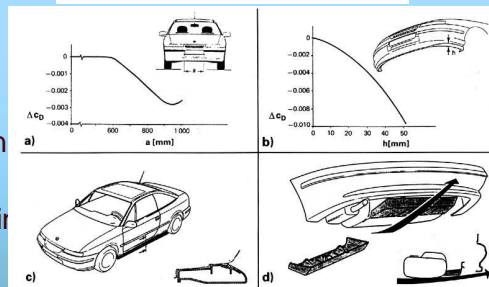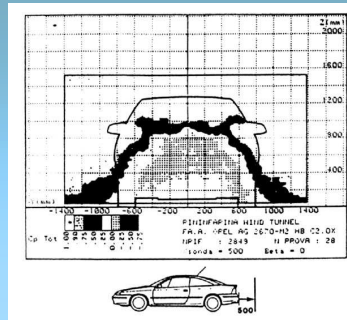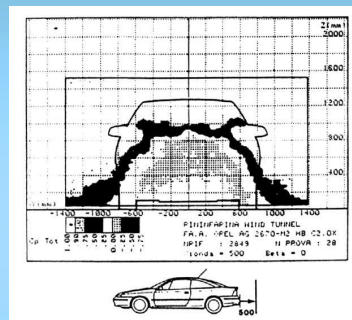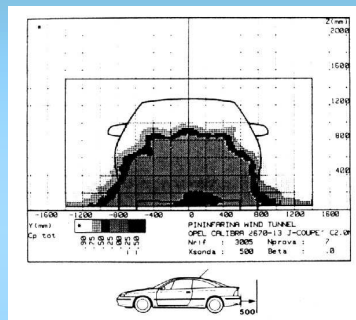 - Lower the door sills

Fig. 4.82 Spoiler development for the Opel Calibra: a) optimum central cutout in the spoiler, b) extended spoiler "corners," c) lowering the door sill, d) improving rear diffuser, after H.-J. EMMELMANN, et al. [4.18].

Before ($c_D \approx 0.28$)   After ($c_D \approx 0.26$)

- Further aerodynamical development
  - Anti-contamination lips
  - Cooling air inlets ($\Delta c_D = 0.014$ for air passing through front end)

40